Original Article

Clinical characteristics and diagnostic challenges of patients with pulmonary actinomycosis: A 10-year experience at a tertiary referral hospital

Sinem Nedime Sökücü[1], Reşit Akyel[2], Fatma Tokgöz Akyıl[1], Seda Tural Önür[1], Kaan Kara[1], Nurdan Şimşek Veske[1], Fatma Elif Çayır Koçal[1], Cengiz Özdemir[3]

ORCID:
Sinem Nedime Sökücü: 0000-0002-7184-2075
Reşit Akyel: 0000-0001-9373-8693
Fatma Tokgöz Akyıl: 0000-0002-3793-9834
Seda Tural Önür: 0000-0002-0657-0392
Kaan Kara: 0000-0001-5896-2497
Nurdan Şimşek Veske: 0000-0001-6817-3416
Fatma Elif Çayır Koçal: 0000-0003-4754-3638
Cengiz Özdemir: 0000-0002-9816-8885

Abstract:

BACKGROUND AND AIM: This study reviews the clinical characteristics, radiological findings, and diagnostic procedures for patients with pulmonary actinomycosis (PA). It also assesses the utility of ^{18}F-fluorodeoxyglucose positron emission tomography-computed tomography (PET-CT) scans in diagnosing PA.

METHODS: Conducted retrospectively at a tertiary referral hospital, this study investigated patients diagnosed with PA between January 2012 and January 2022. Demographics, clinical and radiological findings at presentation, diagnostic steps, PET-CT findings, and the time interval to diagnosis were analyzed.

RESULTS: Among the 34 patients, the mean age at diagnosis was 49 years (range 23–77), with 19 (56%) being male. The most common symptom was cough, reported by 23 patients (68%). Chronic obstructive pulmonary disease and bronchiectasis were the most frequent underlying conditions. Typical chest tomography features included nodular lesions, mass lesions, consolidation, bronchiectasis, and atelectasis. Initial pre-diagnoses included lung cancer in 16 patients (47%), tuberculosis in 9 patients (27%), and late-resolving pneumonia in 6 patients (18%). No patient received an accurate initial diagnosis of PA. All definitive diagnoses were made histopathologically through specimens obtained from: sputum analysis in 1 (2.9%) patient, flexible bronchoscopy in 17 (50%) patients, rigid bronchoscopy in 1 (2.9%) patient, endobronchial ultrasonography in 2 (5.9%) patients, transthoracic needle aspiration in 6 (17.7%) patients, and surgical resection in 7 (20.6%) patients. The mean time from symptom onset to definitive diagnosis was 53.2±44.1 days (Range 9–175 days). Among the patients, 16 (47%) underwent PET-CT, and 10 (29%) underwent cranial magnetic resonance imaging. From the re-assessment of 13 PET-CT scans, the derived values were as follows: Standard Uptake Value (SUV) max value was 6.98±2.74 (range 0.9–9.92), SUV_{mean} value was 3.95±1.51 (range 0.51–5.30), SUV_{peak} value was 5.68±2.24 (range 0.64–7.89), tumor lesion glycolysis was 138.58±151.86 (range 3–440.5), and metabolic tumor volume was 27.85±37.97 (range 0–131.00).

CONCLUSIONS: The diagnosis of PA is challenging and often delayed, frequently misdiagnosed as lung cancer or pulmonary tuberculosis. PA shows moderate metabolic uptake on PET-CT scans and, PET-CT scan is insufficient for accurate and timely differentiation between lung malignancy and PA.

Keywords:

Bronchoscopy, lung cancer, positron emission tomography, pulmonary actinomycosis

[1]Department of Pulmonology, University of Health Sciences, Yedikule Chest Disease and Thoracic Surgery Training and Research Hospital, İstanbul, Türkiye, [2]Department of Nuclear Medicine, University of Health Sciences, Yedikule Chest Disease and Thoracic Surgery Training and Research Hospital, İstanbul, Türkiye [3]Department of Pulmonology, Liv Hospital, Vadi Istanbul

Address for correspondence:
Dr. Sinem Nedime Sökücü, Deparment of Pulmonology, University of Health Sciences, Yedikule Chest Disease and Thoracic Surgery Training and Research Hospital, İstanbul, Türkiye.
E-mail:
sinemtimur@yahoo.com

How to cite this article: Sökücü SN, Akyel R, Tokgöz Akyıl F, Tural Önür S, Kara K, Şimşek Veske N, et al. Clinical characteristics and diagnostic challenges of patients with pulmonary actinomycosis: A 10-year experience at a tertiary referral hospital. Eurasian J Pulmonol 0000;00:1-7.

For reprints contact: kare@karepb.com

Introduction

Pulmonary actinomycosis (PA) is a chronic, uncommon suppurative pulmonary parancyhmal or endobronchial infection primarily caused by Actinomyces israelii–a gram-positive anaerobic saprophytic bacterium known for its branching filaments. This infection typically arises from the aspiration of endogenous oropharyngeal organisms into the lungs. It is commonly observed in individuals with suboptimal oral hygiene or as an extension of cervicofacial infections.[1]

Clinically, PA often presents with nonspecific symptoms such as a productive cough, fever, and bloody sputum. Radiologically, it may exhibit imaging patterns that mimic those of lung malignancies. Although ^{18}F-fluorodeoxyglucose PET-CT is a valuable diagnostic tool for distinguishing between lung malignancies and benign diseases, it has its limitations. False-positive results can arise from conditions such as granulomatous diseases (including sarcoidosis and tuberculosis), abscesses, fungal infections, active thyroiditis, and post surgical changes or radiation.[2]

Current literature on PET-CT findings related to PA primarily consists of case reports, and there is a scarcity of comprehensive studies evaluating these findings.[3] Consequently, the effectiveness of PET CT in differentiating lung malignancy from PA is uncertain.

The primary aim of this study is to assess the clinical and radiological findings in patients diagnosed with PA via histopathological or microbiological means. Additionally, we aim to investigate the potential role of PET-CT findings in the differential diagnosis of PA and lung malignancy.

Materials and Methods

The study is a retrospective, single-center analysis conducted at a tertiary reference hospital specializing in chest diseases. We reviewed hospital records of patients diagnosed with PA from January 2012 to January 2022. Thirty-four patients with PA, confirmed either through histopathologic examination or culture identification, were included.

The study adhered to the ethical principles of the Helsinki Declaration and received approval from Yedikule Chest Disease and Thoracic Surgery Training and Research Hospital's ethics committee (Approval No: 2022-205, dated 10. 03. 2022). Given the retrospective nature of the study, obtaining informed consent from patients was not feasible. However, permission to use patient data anonymously was granted by the hospital. No artificial intelligence-assisted technologies were used in the production of this study.

Recorded parameters and study design

The study comprehensively assessed the following patient parameters: demographics, comorbid diseases, clinical symptoms at presentation, smoking history, chest computed tomography (CT) findings, preliminary diagnosis, diagnostic methods, PET-CT findings, and treatment modalities.

During the diagnostic phase, 16 patients were assessed by PET-CT scans. Of these, 14 patients' PET-CT scans was taken after admission to our hospital while13 scans were re-evaluated by an experienced nuclear medicine physician. This assessment focused on several parameters, including maximum standardized uptake value (SUV_{max}), SUV_{mean}, and SUV_{peak}, which represents an average value within a small, predefined region of interest (ROI) in the tumor. Total lesion glycolysis (TLG) and metabolic tumor volume (MTV) were also calculated. The PET/CT examinations were performed using a Discovery™ IQ system (GE Healthcare, Milwaukee, Brookfield, WI, USA), which features a dedicated four-ring PET scanner. Image analysis was conducted on a vendor-based workstation (GE AW Volume Share 7, GE Medical Systems, Buc, France). The diameter of the lesion was quantified as the lesion diameter in mm divided by the average lesion size. MTV was determined as the total tumor volume exceeding an SUV threshold, and TLG was calculated by multiplying the mean SUV by the MTV. The output results included SUV_{max}, SUV_{mean}, SUV_{peak}, MTV, and corresponding TLG of the lesions, which are used as prognostic markers in lung cancer.[4]

The definitive diagnosis was based on histopathologic identification of Actinomyces colonies or sulfur granules (yellowish clusters of mycelia) or filamentous structures in the tissue specimen, confirmed through Grocott-Gomori methenamine-silver staining.[5]

Statistical analysis

Data analysis was conducted using the Statistical Package for the Social Sciences (SPSS) version 19.0 (SPSS Inc., Chicago, IL, USA). The normality of distribution was assessed for all variables. Continuous variables with normal distributions were presented as mean±standard deviation, while those with non-normal distributions were described

using medians (interquartile range, IQR). Categorical variables were presented as percentages. Independent groups for normally distributed values were compared using the Student's t-test and for non-normally distributed values using the Mann-Whitney U test. Categorical variable comparisons were conducted using the χ^2 test. A significance level of $p<0.05$ was considered statistically significant.

Results

Among the 34 patients evaluated, the mean age at diagnosis was 49 years (range 23–77), with 19 (56%) being male. The most common symptom was cough, occurring in 23 (68%) patients (Table 1). Fifteen patients (44%) had a history of smoking. The most common comorbid conditions were chronic obstructive pulmonary disease and bronchiectasis, each observed in 7 (21%) patients. Other comorbidities included hypertension in 6 (18%) patients, ischemic heart disease and tuberculosis sequelae in 3 (9%) patients each, and congestive heart failure in 1 (3%) patient. Fourteen (41%) patients had no additional diseases.

At initial presentation, the mean C-reactive protein level was 58.7 ± 75.4 mg/L (range 0.3–279), and the mean leucocyte count was 12.3 ± 5.8 10e3/uL (range 4.6–38). The most common findings on chest CT were pulmonary nodules, consolidation, and mass lesions (Table 1). The preliminary diagnosis most frequently considered was lung cancer (n=16, 47%), followed by tuberculosis (n=9, 27%) and late-resolving pneumonia (n=6, 18%). Other initial considerations included bronchiectasis, hypersensitivity pneumonitis, and vasculitis, each in one patient. None of the patients received a correct initial diagnosis.
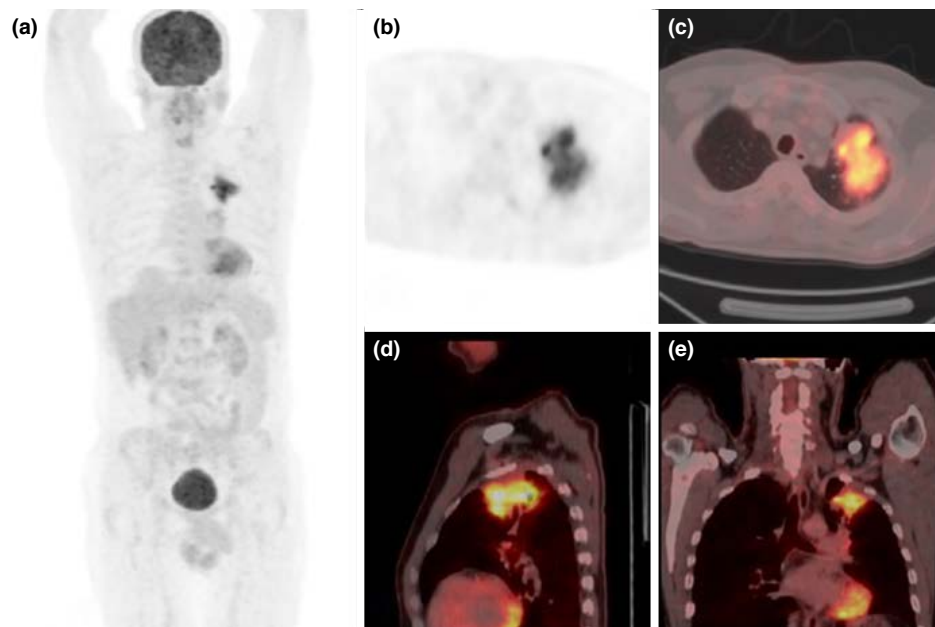
Table 1: Symptoms and chest CT findings at presentation

Symptoms	n	%
Cough	23	68
Sputum expectoration	14	41
Hemoptysis	12	35
Dyspnea	7	21
Weight loss	6	18
Chest pain	5	15
Fever	2	6
Chest CT findings		
Nodular lesions	19	56
Consolidation	16	47
Mass lesion	16	47
Bronchiectasis	11	32
Pleural effusion	9	27
Lymphadenomegaly	9	27
Atelectasis	8	24
Cavitation	5	15
Pleural thickening	4	12
Pericardial effusion	3	9

CT: Computed tomography

Figure 1: (a) Maximum intensity projection (MIP) image displaying a mass in the left upper lobe of the lung. Axial PET (b), and axial (c), sagittal (d), and coronal (e) PET/CT fusion images illustrate a lesion with irregular borders and intense FDG uptake in the apicoposterior segment of the left upper lobe of the lung, which could be mistaken for lung cancer
PET-CT: Positron emission tomography-computed tomography, FDG: Fluorodeoxyglucose

Table 2: Diagnostic work-up and final diagnostic method

Case no	Gender/ age	PET-CT (day)	Days to definitive diagnosis	Non diagnostic procedures	Final diagnostic procedure
1	M/23	–	94	FOB (no EBL)	FOB-TBB
2	M/47	11	91	FOB (no EBL) twice, TTNA by tru-cut	Left lower lobectomy
3	M/59	21	25	–	FOB (no EBL)
4	F/26		43	FOB (no EBL)	Left upper lobectomy
5	M/72	62	77	FOB (no EBL)	TTNA
6	F/50		35	FOB (no EBL) twice	Right lower lobectomy
7	M/51	4	14	TTNA, FOB (no EBL)	TTNA
8	M/67	–	19	FOB (no EBL)	TTNA
9	M/60	1	11	–	TTNA
10	M/64	7	77	–	FOB-mucosal infiltration, biopsy
11	M/47	–	41	–	FOB-mucosal infiltration, biopsy
12	F/25	–	40	–	FOB (no EBL)
13	F/44	–	135	–	FOB (no EBL)
14	M/52	–	35	TTNA	Wedge resection
15	M/51	28	70	FOB-mucosal infiltration, biopsy	FOB-mucosal infiltration, biopsy
16	M/59	–	47	TTNA, TTNA by tru-cut	Left lower lobectomy
17	F/60	–	96	FOB-mucosal infiltration, biopsy	FOB-mucosal infiltration, biopsy
18	F/59	–	9	–	TTNA
19	F/57	152	140	FOB (no EBL), Pleural biopsy	EBUS
20	M/43	127	150	FOB-mucosal infiltration, biopsy	EBUS
21	F/31	7	25	–	TTNA by tru-cut
22	F/39	–	65	–	FOB-mucosal infiltration, biopsy
23	M/44	15	35	FOB (no EBL)	FOB (no EBL)
24	M/60	–	13	–	FOB (no EBL)
25	M/36	–	15	TTNA	FOB (no EBL)
26	M/77	–	11	Sputum cytology	Sputum cytology
27	F/52	1	25	–	FOB (no EBL)
28	M/48	–	175	FOB (no EBL), FOB-mucosal infiltration, biopsy, TTNA	Left pneumonectomy
29	F/26	–	20	FOB (no EBL)	FOB (no EBL)
30	F/52	1	31	–	FOB (no EBL)
31	F/67	1	46	EBUS (from lesion)	FOB (no EBL)
32	F/28	–	20	TTNA	FOB-mucosal infiltration, biopsy
33	F/36	–	17	FOB (no EBL)	Rigid biopsy
34	M/59	–	63	FOB (no EBL)	Left lower lobectomy

PET-CT: Positron emission tomography-computed tomography; m: Male, F: Female, FOB: Fiberoptic bronchoscopy, EBL: Endobronchial lesion, TBB: Transbronchial biopsy, TTNA: Transthoracic needle aspiration

In the context of a preliminary lung cancer diagnosis, 16 (47%) patients underwent an PET-CT scan. The mean SUV_{max} value for the mass lesions in these 16 patients was 6.09±3.22 (range 2.5–12.1) [Fig. 1].

Bronchoscopic evaluation was carried out in 28 (82.35%), with 8 presenting with endobronchial lesions. Table 2 outlines the diagnostic process and final diagnostic methods used. From all the patients sputum analysis was conducted in 13 patients, revealing bacterial colonization in 8 patients, Mycobacterium tuberculosis as co-enfection in 2 patients (6%), and fungal mold in 2 patients (6%). Ten (29%) patients underwent cranial magnetic resonance imaging (MRI). Cranial MRI was requested primarily for a preliminary diagnosis of malignancy in 8 patients and for headache symptoms in 2 patients. The MRI scans identified two cranial lesions in 1 patient: one measuring 12 mm in the right parietal lobe and another 7 mm in the left parietal lobe. Both lesions resolved following appropriate antibiotic therapy.

The final diagnosis of PA was established based on pathologic and/or microbiologic results. Diagnostic specimens were obtained through sputum analysis in 1 (2.9%) patient, flexible bronchoscopy in 17 (50%) patients, rigid bronchoscopy in 1 (2.9%) patient, endobronchial ultrasonography in 2 (5.9%) patients, transthoracic needle aspiration in 6 (17.7%) patients, and surgical resection in 7

Table 3: PET-CT values of lesions related to necrosis

	With Necrosis	Without Necrosis	p
SUV_{max}	7.84±1.52	3.67±4.18	0.412
SUV_{mean}	4.40±0.80	2.10±2.37	0.527
SUV_{peak}	6.53±1.08	2.80±3.25	0.412
TLG	205.00±155.04	22.35±22.23	0.012
MTV	48.00±42.91	4.33±4.41	0.006
Diameter	52.0±7.1	23.0±7.89	0.024

PET-CT: Positron emission tomography-computed tomography; SUV: Standard uptake value, TLG: Total lesion glycolysis, MTV: Metabolic tumor volume

(20.6%) patients. The mean duration from symptom onset to definitive diagnosis was 53.2±44.1 days (range 9–175).

Thirteen PET-CT scans were re-evaluated. There were lesions in the right lung in 7 (54%) patients, in the left lung in 4 (31%) patients, and bilaterally in 2 (15%) patients. The distribution of the lesions was primarily in the upper lobe in 6 (46%) patients, the lower lobe in 2 (15%) patients, the middle lobe in 1 (8%) patient, and multilobar in the remaining patients. Three lesions (23%) showed cavitation, and 7 (53.8%) exhibited necrosis. Upon re-analysis, the lesions' diameters averaged 41.45±22.37 mm (range 10–88), SUV_{max} was 6.98±2.74 (range 0.9–9.92), SUV_{mean} was 3.95±1.51 (range 0.51–5.30), SUV_{peak} was 5.68±2.24 (range 0.64–7.89), TLG was 138.58±151.86 (range 3–440.5), and MTV was 27.85±37.97 (range 0–131.00). The mediastinal pool averaged 1.72±0.32 (ranging from 1.45 to 2.40). No relationship was found between SUV_{max}, SUV_{mean}, SUV_{peak} values and the presence of necrosis. However, both TLG and MTV values were found to be related to necrosis (Table 3).

Discussion

Diagnosing PA can be very challenging due to its nonspecific symptoms and radiological features. In our study, we found that PET-CT does not add significant value to the diagnosis of PA because it exhibits high activity similar to that seen in lung tumors or tuberculosis, which were the most common conditions in the differential diagnosis.

Actinomycosis has a predilection for various organs and systems, with pulmonary involvement being the third most common manifestation. It occurs three times more frequently in men, particularly in the fourth and fifth decades of life.[1] In the largest series of 94 subjects, the mean age for PA was 57.7 years.[6] Consistent with the literature, most of our patients were male (56%) with a mean age of 49 years.

Recent studies highlight that 50% of PA cases can occur in individuals without any pre-existing comorbidities.[7] Factors such as suboptimal oral hygiene and inadequate dental care, as well as chronic lung diseases like emphysema, chronic bronchitis, and bronchiectasis, and a history of previous tuberculosis, are considered risk factors for developing PA.[8] In this respect, our findings were compatible with the recent literature. In our series, 41% of patients had no underlying pathology, and the most common underlying diseases were chronic obstructive pulmonary disease and bronchiectasis.

The clinical spectrum of PA is broad, with the most common respiratory symptoms being cough, sputum production, and chest pain. Other symptoms include dyspnea, hemoptysis, localized chest wall swelling, weight loss, malaise, night sweats, and fewer.[9] In our cohort, cough was the most common symptom, followed by sputum expectoration, hemoptysis, dispnea, weight loss, chest pain, and fever.

The histological identification of yellowish filamentous grains in biopsy material is a distinctive, though not pathognomonic, characteristic indicative of actinomycosis.[1,9] However, this process is rather difficult to master, often causing delays in diagnosing PA. Consistent with the literature, most patients in our series were initially misdiagnosed with lung cancer, tuberculosis, or late-resolving pneumonia. None of the patients in our series received a correct initial diagnosis. In a study by Choi et al.,[3] surgical resection was required for 72.7% of cases, whereas in another series, 50% of 94 patients underwent surgical biopsy.[6] The diagnosis of PA via bronchoscopy has been reported as difficult in many cases. In contrast, in our series, only 20.6% of patients underwent surgery, with bronchoscopy being the most common (52.9%) diagnostic procedure. Despite a lower rate of surgical resection, the duration from symptom onset to definitive diagnosis was relatively long, mean 53.2 days.

There are various radiological presentations of PA. The disease exhibits a spectrum of lung pathologies, ranging from benign infections to mimicking metastatic tumors, which makes reliance solely on imaging modalities insufficient for a definitive diagnosis. Instead, these imaging tools are valuable for guiding the precise location for sampling.[10,11] A characteristic CT feature of parenchymal actinomycosis includes chronic segmental air-space consolidation with necrotic low-attenua-

tion areas, often accompanied by cavity formation and peripheral enhancement.[12] Common chest CT findings in our series included mass lesions, consolidation, and nodular lesions, aligning with the existing literature.

Abnormal fluorodeoxyglucose (FDG) uptake, surpassing the activity expected in normal tissues, was characterized by a standardized uptake value greater than 2.5. This threshold is widely used as an indicator suggestive of malignancy.[13] General PET-CT findings in actinomycosis include intense hypermetabolism similar to that observed in malignancy. In one study, where 6 patients underwent PET-CT, SUV values ranged from 2.1 to 14.3.[14] Another study assessing PET CT findings in 11 patients with confirmed PA found the SUV to be 5.5 (interquartile range, 4.2–8.8). In two recent studies from our country, the median SUV_{max} was recorded at 6.5 and 6.33, respectively.[15,16] These values exceeded the commonly used malignancy threshold of 2.5. Notably, lesions without central necrosis exhibited a higher maximal SUV of 7.5 (interquartile range, 4.9–12.2), compared to those with central necrosis, which had a maximal SUV of 4.8 (interquartile range, 3.2–5.6).[3] Reports from existing literature suggest that the activity of pulmonary actinomycosis can reach as high as 33.1.[17] In parallel to these findings, we detected a mean SUV_{max} value higher then the threshold value of 2.5. The mean SUV_{max} was 6.09±3.22 from 16 PET-CT scan reports, and when 13 were reanalyzed, the SUV_{max} was 6.98±2.74. PET-CT did not facilitate definitive differentiation between PA and malignant lesions. Unlike the study by Choi et al.,[3] we found no significant relation between SUV_{max} value and necrosis. These findings are explained by the elevated metabolic uptake observed on PET CT, suggesting that SUV_{max} may not be a reliable marker for distinguishing between lung malignancy and pulmonary actinomycosis. Recently, other parameters have been proposed to assess the burden of metabolic activity, such as metabolic parameters (SUV_{max}, SUV_{mean}, SUV_{peak}) and volume-based parameters (MTV and TLG).[18] In a series of 125 patients with non-small cell lung cancer (NCLC), 75 adenocarcinoma tumors had a median SUV_{max} of 9.30, MTV of 28.56, and TLG of 109.25, whereas 50 patients with squamous cell carcinoma tumors had a median SUV_{max} of 15.50, MTV of 42.35, and TLG of 380.48.[19] In our series, the SUV_{max} value was 6.98, SUV_{mean} was 3.95, SUV_{peak} was 5.68, TLG was 138.58, and MTV was 27.85±37.97. Volumetric parameters such as MTV and TLG were additionally employed to characterize disease burden and tumor aggressiveness in NSCLC. Furthermore, a meta-analysis showed that elevated values of SUV_{max}, MTV, and TLG were predictive of a heightened risk of recurrence or mortality in patients diagnosed with NSCLC.[20] Although SUV_{max} is a standard parameter in clinical practice, other metrics are not yet widely adopted, mainly due to a lack of consensus on the optimal method for lesion segmentation in FDG PET imaging. Current routine clinical practices have limitations in distinguishing lung malignancy from pulmonary actinomycosis, highlighting the need for further research in this area.

In our review of the literature, we find that the brain is occasionally affected secondarily by actinomycosis. Notably, a case report detailing two instances of brain involvement demonstrated that cranial MRI scans conducted in the third month of treatment showed either partial or complete resolution of symptoms.[21] In our study, 29.4% of the patients underwent cranial MRI evaluations. In one of these cases, lesions suspected to be malignant were identified, but they resolved following appropriate antibiotic therapy.

There are certain limitations to our study. It was conducted at a single-center; however, this center is a referral center in our country, which means it receives severe cases from across the nation. Another limitation is the relatively low number of patients undergoing PET-CT. Nonetheless, it is important to note that our study is the first to specifically evaluate all the metabolic and volumetric parameters of PET-CT scans. We believe our findings significantly contribute to the literature by promoting more accurate diagnosis of PA, a condition that commonly suffers from delays and flaws in the diagnostic process.

Conclusion

Pulmonary actinomycosis, a bacterial infection, is frequently misdiagnosed as lung cancer or pulmonary tuberculosis due to its nonspecific symptoms and radiological similarities. Diagnosing this condition is challenging and time-consuming. Given the elevated metabolic uptake observed in pulmonary actinomycosis on PET CT, this imaging technique may not be helpful in distinguishing lung malignancy from pulmonary actinomycosis. Considering the common occurrence of false positives for other inflammatory diseases on PET-CT, it is crucial to include PA in the differential diagnosis, especially in cases that present as positive on FDG-PET.

References

1. Valour F, Sénéchal A, Dupieux C, Karsenty J, Lustig S, Breton P, et al. Actinomycosis: etiology, clinical features, diagnosis, treatment, and management. Infect Drug Resist 2014;7:183–97.

2. Almuhaideb A, Papathanasiou N, Bomanji J. 18F-FDG PET/CT imaging in oncology. Ann Saudi Med 2011;31(1):3–13.

3. Choi H, Lee H, Jeong SH, Um SW, Kown OJ, Kim H. Pulmonary actinomycosis mimicking lung cancer on positron emission tomography. Ann Thorac Med 2017;12(2):121–4.

4. Li X, Wang D, Yu L. Prognostic and Predictive Values of Metabolic Parameters of 18F-FDG PET/CT in Patients With Non-Small Cell Lung Cancer Treated With Chemotherapy. Mol Imaging 2019;18:1536012119846025.

5. Pine L. Actinomyces and microaerophilic actinomycetes. In: Braude AI, Davis CE, Fierer J, eds. Medical microbiology and infectious diseases. Philadelphia, PA: Saunders; 1981. p.448.

6. Kim SR, Jung LY, Oh IJ, Kim YC, Shin KC, Lee MK, et al. Pulmonary actinomycosis during the first decade of 21st century: cases of 94 patients. BMC Infect Dis 2013;13:216.

7. Khaled D, Besma T, Kamel A, Rachid B. Pulmonary Actinomycosis Revealed by a Solitary Pulmonary Nodule. Case Rep Pulmonol 2022;2022:7877729.

8. BATES M, CRUICKSHANK G. Thoracic actinomycosis. Thorax 1957;12(2):99–124.

9. Mabeza GF, Macfarlane J. Pulmonary actinomycosis. Eur Respir J 2003;21(3):545–51.

10. Allen HA 3rd, Scatarige JC, Kim MH. Actinomycosis: CT findings in six patients. AJR Am J Roentgenol 1987;149(6):1255–8.

11. Ng KK, Cheng YF, Ko SF, Ng SH, Pai SC, Tsai CC. CT findings of pediatric thoracic actinomycosis: report of four cases. J Formos Med Assoc 1992;91(3):346–50.

12. Kim TS, Han J, Koh WJ, Choi JC, Chung MJ, Lee JH, et al. Thoracic actinomycosis: CT features with histopathologic correlation. AJR Am J Roentgenol 2006;186(1):225–31.

13. Hong R, Halama J, Bova D, Sethi A, Emami B. Correlation of PET standard uptake value and CT window-level thresholds for target delineation in CT-based radiation treatment planning. Int J Radiat Oncol Biol Phys 2007;67(3):720–6.

14. Sun XF, Wang P, Liu HR, Shi JH. A Retrospective Study of Pulmonary Actinomycosis in a Single Institution in China. Chin Med J 2015;128(12):1607–10.

15. Hoca NT, Berktaş MB, Söyler Y, Celep C, Tanrıkulu FB. Clinical features and treatment outcomes of pulmonary actinomycosis. Eur Rev Med Pharmacol Sci 2022;26(21):8064–72.

16. Baykal H, Ulger AF, Çelik D, Tanrikulu FB, Tatci E. Clinical and radiological characteristics of pulmonary actinomycosis mimicking lung malignancy. Rev Assoc Med Bras (1992) 2022;68(3):372–6.

17. Hoekstra CJ, Hoekstra OS, Teengs JP, Postmus PE, Smit EF. Thoracic actinomycosis imaging with fluorine-18 fluorodeoxyglucose positron emission tomography. Clin Nucl Med 1999;24(7):529–30.

18. Im HJ, Bradshaw T, Solaiyappan M, Cho SY. Current Methods to Define Metabolic Tumor Volume in Positron Emission Tomography: Which One is Better? Nucl Med Mol Imaging 2018;52(1):5–15.

19. Behgam Shadmehr M, Khosravi A, Abbasi Dezfouli A, Bakhshayesh-Karam M, Jamaati H, Doroudinia A, et al. Clinical Significance of Quantitative FDG PET/CT Parameters in Non-Small Cell Lung Cancer Patients. Tanaffos 2020;19(3):186–94.

20. Liu J, Dong M, Sun X, Li W, Xing L, Yu J. Prognostic Value of 18F-FDG PET/CT in Surgical Non-Small Cell Lung Cancer: A Meta-Analysis. PLoS One 2016;11(1):e0146195.

21. Mohindra S, Savardekar A, Rane S. Intracranial actinomycosis: varied clinical and radiologic presentations in two cases. Neurol India 2012;60(3):325–7.